Eur. Phys. J. B **12**, 351–365 (1999)

THE EUROPEAN PHYSICAL JOURNAL B

EDP Sciences

Spin susceptibility of interacting electrons in one dimension: Luttinger liquid and lattice effects

H. Nélisse[1], C. Bourbonnais[1,2,a], H. Touchette[1], Y.M. Vilk[3], and A.-M.S. Tremblay[1,2]

[1] Département de physique et Centre de recherche en physique du solide, Université de Sherbrooke, Sherbrooke, Quebec, Canada J1K 2R1
[2] Institut canadien de recherches avancées, Université de Sherbrooke, Sherbrooke, Québec, Canada J1K 2R1
[3] 2100 Valencia Dr. apt. 406, Northbrook, IL 60062, U.S.A.

Received 2 March 1999

Abstract. The temperature-dependent uniform magnetic susceptibility of interacting electrons in one dimension is calculated using several methods. At low temperature, the renormalization group reveals that the Luttinger liquid spin susceptibility $\chi(T)$ approaches zero temperature with an infinite slope in striking contrast with the Fermi liquid result and with the behavior of the compressibility in the absence of umklapp scattering. This effect comes from the leading marginally irrelevant operator, in analogy with the Heisenberg spin 1/2 antiferromagnetic chain. Comparisons with Monte Carlo simulations at higher temperature reveal that non-logarithmic terms are important in that regime. These contributions are evaluated from an effective interaction that includes the same set of diagrams as those that give the leading logarithmic terms in the renormalization group approach. Comments on the third law of thermodynamics as well as reasons for the failure of approaches that work in higher dimensions are given.

PACS. 71.10.Pm Fermions in reduced dimensions (anyons, composite fermions, Luttinger liquid, etc.) – 71.10.Fd Lattice fermion models (Hubbard model, etc.) – 75.40.Mg Numerical simulation studies

1 Introduction

There are a number of organic conductors, including the Bechgaard salts for example, for which the distinctive behavior of one-dimensional interacting electrons is observed over a wide range of temperature [1,2]. Among the characteristics observed is the asymptotic low-frequency, long-wavelength electronic behavior which, in one dimension, belongs to the universality class of Luttinger liquids. This universality class plays in one-dimension the role of Landau Fermi liquid theory in higher dimension, providing a framework to understand the occurrence of power law behavior, spin-charge separation and various other characteristics of one-dimensional systems [3].

While much is known about the predictions of Luttinger liquid theory, non-singular quantities, such as the uniform magnetic spin susceptibility χ, are not completely understood theoretically. Experimentally, $\chi(T)$ can be accurately measured as a function of temperature using a number of techniques, including Knight shift in Nuclear Magnetic Resonance (NMR) experiments. In higher dimension, the theoretical situation for $\chi(T)$ is clear within Landau Fermi liquid theory. The prediction for this key quantity is a Pauli-like susceptibility whose absolute value is enhanced by interactions. For Luttinger liquid theory in one dimension pioneering work was done by Dzyaloshinskii and Larkin [4] and by Lee *et al.* [5] A few years ago, Bourbonnais [6], using the renormalization group, readdressed this problem. The conclusion that emerges from these works is that the temperature dependence of $\chi(T)$ remains important up to $T = 0$, contrary to the Fermi liquid result in high dimension where temperature dependence shows up only on the scale of the Fermi energy. The renormalization group approach is expected to give the correct asymptotic low-temperature behavior of the Luttinger liquid. To obtain quantitative confirmation of these results from a specific microscopic model, it is customary to study the Hubbard model that has an exact Bethe *ansatz* solution in one dimension and belongs to the Luttinger-liquid universality class. Despite the exact solution, the Bethe *ansatz* magnetic susceptibility must be computed numerically [7]. Additional results have been obtained recently by Jüttner *et al.* [8] through a quantum transfer matrix method, by Mila and Penc through world line quantum Monte Carlo simulations [9], and by Moukouri [10] through Density Matrix Renormalization Group techniques. It is important to notice that the low temperature limit is difficult to reach numerically using any of the available numerical approaches, including Bethe *ansatz*.

In this paper, following references [6,11], we derive the renormalization group (RG) prediction for the

[a] e-mail: cbourbon@physique.usherb.ca

temperature-dependent uniform magnetic susceptibility of the g-ology Hamiltonian. We show that the uniform magnetic susceptibility $\chi(T)$ of this Luttinger liquid approaches zero temperature with an infinite slope, in analogy with the spin 1/2 antiferromagnetic Heisenberg chain [12,13]. This effect comes from backscattering of right- and left-moving electrons, which is the leading marginally irrelevant operator. We show that this phenomenon appears in a temperature range where no numerical calculation has been done yet. We also obtain predictions at higher temperature by using numerical simulations done on the Hubbard Hamiltonian at quarter filling. To obtain *quantitative* agreement with the simulations, we find it necessary to include non-logarithmic contributions that are beyond the RG treatment. This is done by using an approach inspired from the Kanamori [14]-Brueckner [15] theory valid in higher dimension [16]. The subset of diagrams that must be resummed in one dimension is suggested by the RG and it does differ from the subset used in higher dimension. The reasons for the failure of higher-dimensional approaches are also discussed.

The g-ology and Hubbard Hamiltonians are introduced in Section 2. In Section 3, we present the results of numerical calculations and in Section 4 the RG calculation, including the prediction of the infinite slope as $T \to 0$. Section 5 discusses the comparison between numerical results, RG prediction and the reasons for the failure of higher-dimensional approaches. We conclude with a summary of our main results and general comments on the range of applicability of Luttinger-liquid theory.

2 Hubbard model and connection with G-ology

The simulations are done for the Hubbard model

$$H = -t \sum_{<ij>\sigma} \left(c^\dagger_{i\sigma} c_{j\sigma} + c^\dagger_{j\sigma} c_{i\sigma} \right) + U \sum_i n_{i\uparrow} n_{i\downarrow} \qquad (1)$$

where units of energy are chosen such that the hopping matrix element t equals unity in the simulations. The creation (annihilation) operators $c^\dagger_{i\sigma}$ ($c_{i\sigma}$) create (annihilate) electrons of spin σ in the orbital located on site i with position r_i. Only nearest-neighbor hopping is allowed. The last term, with the usual occupation number operators $n_{i\uparrow} = c^\dagger_{i\sigma} c_{i\sigma}$, represents the short-range repulsion U, felt by the electrons when they occupy the same orbital at site i.

As is well known [17], there are logarithmic divergences in the perturbative treatment of the Hubbard model in one dimension. These can be handled directly by infinite resummations of parquet diagrams [17], or most easily by a renormalization group treatment [18–21]. In this case, the Hubbard Hamiltonian is not a fixed-point Hamiltonian. It is necessary to consider the renormalization group flows in a more general space of Hamiltonians called g-ology Hamiltonian. In the rest of this section, we recall how to cast the Hubbard Hamiltonian as a special case of g-ology. First, it is useful to rewrite it in the form

$$H = -t \sum_{<ij>\sigma} \left(c^\dagger_{i\sigma} c_{j\sigma} + c^\dagger_{j\sigma} c_{i\sigma} \right) + \frac{U}{2} \sum_{i\sigma\sigma'} c^\dagger_{i\sigma} c^\dagger_{i\sigma'} c_{i\sigma'} c_{i\sigma} \qquad (2)$$

which, compared with equation (1), contains an additional term that can be absorbed in a chemical potential shift. The g-ology Hamiltonian being defined in Fourier space, we take

$$c_\sigma(k) = \frac{1}{\sqrt{L}} \sum_{j=1}^{L} \mathrm{e}^{-\mathrm{i}kr_j} c_{j\sigma} \quad ; \quad c^\dagger_\sigma(k) = \frac{1}{\sqrt{L}} \sum_{j=1}^{L} \mathrm{e}^{\mathrm{i}kr_j} c^\dagger_{j\sigma} \qquad (3)$$

where we have chosen unity for the lattice spacing so that the number of sites and the system size are both equal to L. Using these variables, and neglecting *umklapp* processes, we can write,

$$H = \sum_{k,\sigma} (-2t \cos k)\, c^\dagger_\sigma(k)\, c_\sigma(k) + \frac{U}{2L} \times \sum_{k,k',q,\sigma,\sigma'} c^\dagger_\sigma(k)\, c^\dagger_{\sigma'}(k')\, c_{\sigma'}(k'+q)\, c_\sigma(k-q). \qquad (4)$$

In recent versions of the renormalization group [13], the full cosine dispersion relation can be taken into account, but in the more usual version that we consider here, the dispersion relation is linearized around the two Fermi points $\pm k_\mathrm{F}$, and one considers only scatterings around and between these points. To rewrite the Hubbard Hamiltonian equation (4) in a way that highlights the processes that are allowed by the Pauli principle, the sum over momentum transfers q is divided also in three pieces: $q \approx 0$, and $q \approx \pm 2k_\mathrm{F}$. Furthermore, one introduces a lower index p to the creation-annihilation operators that, for the moment, just indicates if the allowed particle momenta are mostly around the $+k_\mathrm{F}$ Fermi point (right-moving (+)), or around the $-k_\mathrm{F}$ Fermi point or (left-moving (−)). This rearrangement gives, after one allows the k sums to run from $-k_0 + pk_\mathrm{F}$ to $k_0 + pk_\mathrm{F}$ with k_0 a cut-off wave vector of the order of k_F.

see equation (5) next page

where the linearized dispersion relation is

$$\epsilon_p(k) = p v_\mathrm{F} (k - p k_\mathrm{F}) \quad ; \quad v_\mathrm{F} \equiv 2t \sin k_\mathrm{F}. \qquad (6)$$

The restrictions on momentum transfer q should normally be set to avoid double counting various scattering processes. However, it is simpler to introduce additional states that linearly extrapolate the right and left-moving electron dispersion relations. In otherwords, strictly speaking we should have $c_{+,\sigma}(k) = c_\sigma(k)$ for $0 \le k < \pi$ and $c_{-,\sigma}(k) = c_\sigma(k)$ for $-\pi \le k < 0$ while, instead, we add states in such a way k runs from $-\infty$ to $+\infty$ for both cases $p = \pm 1$. Each of these sets, $p = \pm 1$, are defined as a "branch" with the corresponding dispersion relation $\epsilon_p(k) = p v_\mathrm{F}(k - p k_\mathrm{F})$. The added unphysical states should not contribute appreciably because of the large energy denominators, the Pauli principle and the cut-offs

$$
\begin{aligned}
H \approx & \sum_{k,\sigma,p} \epsilon_p(k)\, c^{\dagger}_{p,\sigma}(k)\, c_{p,\sigma}(k) \\
& + \frac{U}{2L} \sum_{\sigma,\sigma'=\uparrow}^{\downarrow} \sum_{(p,p'=\pm)} \sum_{(k=-k_0+pk_{\mathrm{F}})}^{k_0+pk_{\mathrm{F}}} \sum_{(k'=-k_0+p'k_{\mathrm{F}})}^{k_0+p'k_{\mathrm{F}}} \sum_{q} c^{\dagger}_{p,\sigma}(k)\, c^{\dagger}_{p',\sigma'}(k')\, c_{p',\sigma'}(k'+q)\, c_{p,\sigma}(k-q) \\
& + \frac{U}{2L} \sum_{\sigma,\sigma'=\uparrow}^{\downarrow} \sum_{(k=-k_0+k_{\mathrm{F}})}^{k_0+k_{\mathrm{F}}} \sum_{(k'=-k_0-k_{\mathrm{F}})}^{k_0-k_{\mathrm{F}}} \sum_{q} c^{\dagger}_{+,\sigma}(k)\, c^{\dagger}_{-,\sigma'}(k')\, c_{+,\sigma'}(k'+q+2k_{\mathrm{F}})\, c_{-,\sigma}(k-q-2k_{\mathrm{F}}) \\
& + \frac{U}{2L} \sum_{\sigma,\sigma'=\uparrow}^{\downarrow} \sum_{(k'=-k_0+k_{\mathrm{F}})}^{k_0+k_{\mathrm{F}}} \sum_{(k=-k_0-k_{\mathrm{F}})}^{k_0-k_{\mathrm{F}}} \sum_{q} c^{\dagger}_{-,\sigma}(k)\, c^{\dagger}_{+,\sigma'}(k')\, c_{-,\sigma'}(k'+q-2k_{\mathrm{F}})\, c_{+,\sigma}(k-q+2k_{\mathrm{F}}) \qquad (5)
\end{aligned}
$$

in the sums over k and k' that regularize perturbation theory. Hence, in the weak to intermediate coupling regime only scatterings near the Fermi surface are important so we can assume that the sum over q that is left for each of the three pieces is free to run from $-\infty$ to $+\infty$. In the g-ology notation, the last two terms of equation (5) are regrouped into $2k_{\mathrm{F}}$ scatterings with an interaction constant g_1, while the first interaction term is divided into $q \approx 0$ scatterings on the same branch (g_4), and $q \approx 0$ scatterings between two different branches (g_2), namely

see equation (7) next page

In this notation then, the space of parameters is closed under the renormalization-group (RG) induced flow.

The Hubbard Hamiltonian and the above g-ology Hamiltonian clearly differ since the dispersion relation is linearized and g-ology contains fewer scattering terms than the original Hubbard model. If one assumes that the high-energy processes that were dropped do not influence the Physics, then $g_1 = g_2 = g_4 = U$ for the Hubbard model. It is important to notice, however, that this identification is an approximation. In fact the g-ology Hamiltonian H_g is a small-cut-off limit of the Hubbard model and is strictly related to the Hubbard model only in a RG sense. Generally, the appropriate initial values of the coupling constants entering the RG would be such that, for example, $g_4 \neq U$. Here by rotational invariance parallel and perpendicular components of the coupling constant g_1 are identical, a property that is preserved by the RG transformation on the g-ology Hamiltonian.

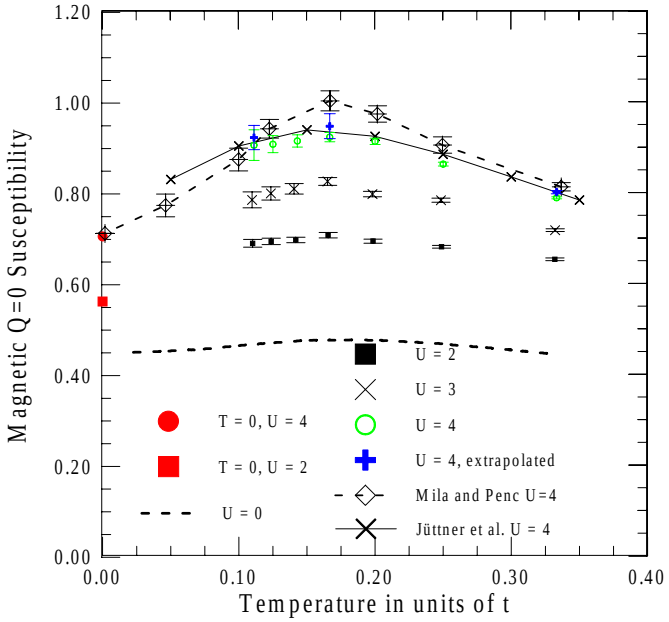

Fig. 1. Monte Carlo simulation results for the temperature dependent susceptibility as defined by equation (8) and $T\chi = S(q=0)$. Our Monte Carlo results (2×10^5 measurements) are shown by symbols with error bars for different values of U. For $U = 4$ the extrapolation of our results to $\Delta\tau = 0$ is also shown for three temperatures. They are, within error bars, in agreement with the quantum transfer matrix results of Jüttner *et al.* [8] shown by the solid line. Points joined by the dashed line are from reference [9] while the zero-temperature results shown by symbols are from Shiba [22].

3 Quantum Monte Carlo results

We are interested in the quarter-filled case, which corresponds to a large class of organic conductors. Earlier results for the uniform magnetic susceptibility χ include the following. First, zero temperature results that have been obtained from the Bethe ansatz by Shiba [22] and are shown for $U/t = 2$, and $U/t = 4$ as the left-most points in Figure 1. Recently, Jüttner *et al.* [8] used a new approach based on the Trotter-Suzuki mapping and a subsequent investigation of the quantum transfer matrix to obtain the temperature-dependent results shown by the solid line in Figure 1. Earlier results had been obtained using a world line algorithm by Mila and Penc [9]. The corresponding results at $U/t = 4$ are linked by a dashed line in Figure 1. These results disagree substantially from those of Jüttner *et al.* [8]. As we show below, our Monte Carlo simulations confirm the latter results. The calculations of reference [9] are probably less accurate because they were obtained not only from the usual extrapolations to $\Delta\tau = 0$ and $L = \infty$, they also required extrapolation to $q = 0$ of the finite wave vector results because the world-line algorithm is for the canonical ensemble. Finite-temperature DMRG calculations [10] cannot yet reach sizes large enough to be

$$
\begin{aligned}
H_g = & \sum_{k,\sigma,p} \epsilon_p(k)\, c^\dagger_{p,\sigma}(k)\, c_{p,\sigma}(k) \\
& + \frac{g_1}{2L} \sum_q \sum_{\sigma,\sigma'=\uparrow}^{\downarrow} \sum_{p=\pm} \sum_{(k=-k_0+pk_\mathrm{F})}^{k_0+pk_\mathrm{F}} \sum_{(k'=-k_0-pk_\mathrm{F})}^{k_0-pk_\mathrm{F}} c^\dagger_{p,\sigma}(k)\, c^\dagger_{-p,\sigma'}(k')\, c_{p,\sigma'}(k'+q+2pk_\mathrm{F})\, c_{-p,\sigma}(k-q-2pk_\mathrm{F}) \\
& + \frac{g_2}{2L} \sum_q \sum_{\sigma,\sigma'=\uparrow}^{\downarrow} \sum_{p=\pm} \sum_{(k=-k_0+pk_\mathrm{F})}^{k_0+pk_\mathrm{F}} \sum_{(k'=-k_0-pk_\mathrm{F})}^{k_0-pk_\mathrm{F}} c^\dagger_{p,\sigma}(k)\, c^\dagger_{-p,\sigma'}(k')\, c_{-p,\sigma'}(k'+q)\, c_{p,\sigma}(k-q) \\
& + \frac{g_4}{2L} \sum_q \sum_{\sigma,\sigma'=\uparrow}^{\downarrow} \sum_{p=\pm} \sum_{(k=-k_0+pk_\mathrm{F})}^{k_0+pk_\mathrm{F}} \sum_{(k'=-k_0+pk_\mathrm{F})}^{k_0+pk_\mathrm{F}} c^\dagger_{p,\sigma}(k)\, c^\dagger_{p,\sigma'}(k')\, c_{p,\sigma'}(k'+q)\, c_{p,\sigma}(k-q)\,. \qquad (7)
\end{aligned}
$$

compared with the results of Figure 1, although for larger values of the interaction it would be possible.

We have used the so-called determinantal Monte Carlo method (BSS algorithm) [23] to obtain the other finite-temperature results in Figure 1 for $U/t = 2, 3, 4$. Since equal-time quantities give better statistics, the quantity that was computed is the magnetic structure factor for an L site lattice

$$S(q) = \frac{1}{L} \sum_{\mathbf{r}_i, \mathbf{r}_j} \exp\left[\mathrm{i}q\,(r_i - r_j)\right] \langle (n_{i,\uparrow} - n_{i,\downarrow})\,(n_{j,\uparrow} - n_{j,\downarrow}) \rangle\,. \qquad (8)$$

This quantity at $q = 0$ is trivially related to the magnetic susceptibility through the fluctuation-dissipation theorem ($S(0) = T\chi$). The results shown by isolated points with error bars in Figure 1 are for a 30 site chain at quarter-filling. The units are chosen so that $t = 1$. About 2×10^5 measurements were taken for each point. For $U = 4$ and three temperatures, namely $T = 1/3$, $1/6$ and $1/9$, we have done the extrapolation to $\Delta\tau = 0$ using three values of $\Delta\tau$. These results are plotted as crosses in Figure 1. Our extrapolated results are in excellent agreement with those of Jüttner *et al.* [8], while our unextrapolated results systematically underestimate those of Jüttner *et al.* [8] by at most a few percent at the highest temperatures. We conclude that the discretization step that we used in imaginary time, $\Delta\tau = 1/8$, leads to a systematic underestimation (of order $(\Delta\tau)^2$) [24] of the susceptibility which is smaller than the statistical error on the figure except perhaps for the two highest temperatures where the extrapolated results are within two error bars of the unextrapolated ones.

As we shall see in the RG treatment, interactions cause a singularity in the temperature derivative of the $q = 0$ susceptibility at $T = 0$. Observation of this singularity would require huge system sizes. However, at higher temperature, where the susceptibility is regular, finite-size effects should be negligible when the thermal de Broglie wavelength $\xi_\mathrm{th} = v_\mathrm{F}/(\pi T)$ is smaller than the system size. For system sizes 30 and quarter-filling, this criterion means that finite-size effects should be small for $T > 0.02$. In fact, for the lowest temperature we have considered $T \approx 0.1$, we have $\xi_\mathrm{th} \approx 5$. We have verified for $T > 0.1$ that indeed our results are the same, within statistical accuracy, for sizes $10, 20, 30, 40$.

The results shown in Figure 1 do not contain the factor $1/2$ for each external spin vertex, hence they are larger by a factor of four than those defined in the following section.

4 Renormalization group approach

The renormalization group provides a useful tool to understand the g-ology Hamiltonian and its fixed point behavior, the Luttinger liquid. In the first subsection, we summarize well known results for the renormalization group flow of the parameters [18–21]. In the second subsection, we show how to apply perturbative techniques to the small cut-off theory to compute the uniform magnetic spin susceptibility.

4.1 Renormalization group

Following the Kadanoff-Wilson renormalization group procedure of reference [21] we derive the one-dimensional scaling results that are essential for the calculation of the magnetic susceptibility. One starts with the partition function of the one-dimensional electron gas expressed in terms of a functional integral over anticommuting fields, namely

$$Z = \int\int D\psi^* D\psi\, \mathrm{e}^{S[\psi^*,\psi]}. \qquad (9)$$

The Euclidean action $S = S^0 + S_I$ corresponding to the g-ology Hamiltonian (7), consists in a sum of free and interacting parts. Using the definition

$$\psi_{p,\sigma}(k, \mathrm{i}k_n) = \sqrt{\frac{T}{L}} \sum_{j=1}^{L} \int_0^\beta \mathrm{d}\tau \mathrm{e}^{-\mathrm{i}kr_j + \mathrm{i}k_n\tau} \psi_{p,\sigma}(r_j, \tau) \quad (10)$$

with the fermionic Matsubara frequencies $k_n = (2n+1)\,\pi T$, $n = 0, \pm1, \pm2, ...$ and the notations $\widetilde{k} = [k, k_n = (2n+1)\pi T]$ and $\widetilde{q} = (q, \mathrm{i}q_m = 2m\pi T)$ the two parts of the action are given by

$$S^0[\psi^*, \psi] = \sum_{p,\widetilde{k},\sigma} G_p^{0-1}(\widetilde{k}) \psi^*_{p,\sigma}(\widetilde{k}) \psi_{p,\sigma}(\widetilde{k}) \qquad (11)$$

and

$$S_I[\psi^*,\psi] = \frac{T}{2L}\sum_{\{\ p,\widetilde{k}_1,\widetilde{k}_2,\widetilde{q},\sigma\}} (g_1\delta_{\sigma_1\sigma_3}\delta_{\sigma_2\sigma_4} - g_2\delta_{\sigma_1\sigma_4}\delta_{\sigma_2\sigma_3})$$

$$\times\psi^*_{p,\sigma_1}\left(\widetilde{k}_1\right)\psi^*_{-p,\sigma_2}(\widetilde{k}_2)\psi_{-p,\sigma_3}(\widetilde{k}_2+\widetilde{q})\psi_{p,\sigma_4}(\widetilde{k}_1-\widetilde{q})$$

$$-\frac{T}{2L}\sum_{\{\ p,\widetilde{k}_1,\widetilde{k}_2,\widetilde{q},\sigma,\sigma'\}} g_4\ \psi^*_{p,\sigma}(\widetilde{k}_1)\psi^*_{p,\sigma\prime}(\widetilde{k}_2)$$

$$\times\psi_{p,\sigma\prime}(\widetilde{k}_2+\widetilde{q})\psi_{p,\sigma}(\widetilde{k}_1-\widetilde{q}). \qquad (12)$$

To rewrite this equation, the g_1 term in equation (7) has been subjected to the change of variable, $q \to k - k' - 2pk_{\rm F} - q$. In the usual g-ology terminology described above, the constants g_1 and g_2 stand for the backward and forward coupling constants between right and left moving carriers whereas g_4 is the forward scattering amplitude for electrons on the same branch. The sums over wave vectors in $S_I[\psi^*,\psi]$ are restricted by the bandwidth cut-off $E_0 = 2v_{\rm F}k_0$. The measure is given by

$$D\psi^*D\psi = \prod_{p,\sigma,\widetilde{k}} d\psi^*_{p,\sigma}(\widetilde{k})d\psi_{p,\sigma}(\widetilde{k}) \qquad (13)$$

while the one-dimensional free propagator of the fermion field has the form

$$G^0_p(\widetilde{k}) = -\left\langle\psi_{p,\sigma}\left(\widetilde{k}\right)\psi^*_{p,\sigma}\left(\widetilde{k}\right)\right\rangle_0 = \frac{1}{\mathrm{i}k_n - \epsilon_p\left(k\right)} \qquad (14)$$

with $\epsilon_p(k)$ as in equation (6).

In the bandwidth cut-off scheme, the renormalization group procedure in one dimension consists in successive partial integrations of fermion degrees freedom in the outer band-momentum shell corresponding to energies $\frac{1}{2}E_0(l) \geq \epsilon_p(k) > \frac{1}{2}E_0(l+dl)$ for electrons and $-\frac{1}{2}E_0(l) \leq \epsilon_p(k) < -\frac{1}{2}E_0(l+dl)$ for holes, with $E_0(l) = E_0\mathrm{e}^{-l}$ an effective bandwidth cut-off at step $l \geq 0$ $(E_0 \equiv 2E_{\rm F})$. For each partial summation, a complete Matsubara frequency sum is performed. Making use of the linked cluster theorem, the partial trace can be formally written as

$$Z \propto \iint_< D\psi^*D\psi\mathrm{e}^{S[\psi^*,\psi]_\ell}$$

$$\times \iint D\overline{\psi}^*D\overline{\psi}\mathrm{e}^{S_0[\overline{\psi}^*,\overline{\psi}]+S_I[\overline{\psi}^*,\overline{\psi},\psi^*,\psi]}$$

$$\propto Z_{\overline{0}}\iint_< D\psi^*D\psi\mathrm{e}^{S[\psi^*,\psi]_\ell}$$

$$\times\exp\left(\sum_{n=1}^{\infty}\frac{1}{n!}\left\langle\left(S_I\left[\overline{\psi}^*,\overline{\psi},\psi^*,\psi\right]\right)^n\right\rangle_{\overline{0},c}\right) \qquad (15)$$

$$\propto \iint_< D\psi^*D\psi\mathrm{e}^{S[\psi^*,\psi]_{\ell+d\ell}}. \qquad (16)$$

Here the $\overline{\psi}'s$ refer to fermion fields with a band wave vector in the outer momentum shell while the $\psi' s$ pertain to lower momentum degrees of freedom that are kept fixed. The outer shell averages (connected diagrams) are defined with respect to the free part $S^0[\overline{\psi}^*,\overline{\psi}]$. The Hartree-Fock diagrams redefine the chemical potential in such a way that Luttinger's Fermi surface [25] is preserved. At the one-loop level, the renormalization of g_1 and g_2 is obtained from the evaluation of the $n = 2$ outer-shell averages where

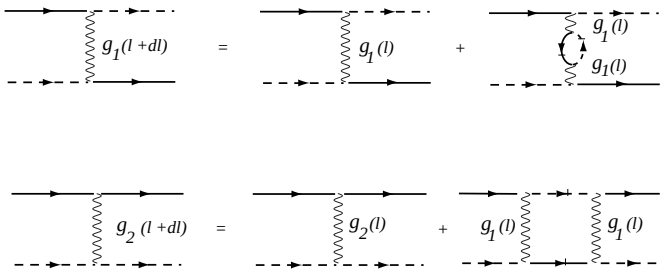

Fig. 2. Non-cancelling diagrams for the renormalization group calculation of the recursion relations for g_1 and g_2. Wiggly lines are for interactions, dashed (solid) lines are for fermions on the left $-k_{\rm F}$ (right $k_{\rm F}$) branch of the spectrum. The bar on a line indicates that the corresponding integration is in the small momentum shell being integrated.

$$S_I[\overline{\psi}^*,\overline{\psi},\psi^*,\psi] \sim\ \overline{\psi}^*_p\overline{\psi}^*_{-p}\psi_{-p}\psi_p +\ \overline{\psi}^*_p\overline{\psi}_{-p}\psi^*_{-p}\psi_p + ... \qquad (17)$$

corresponding to outer-shell decompositions in the Cooper, and Peierls channels. An essential characteristic of the one-dimensional electron gas that emerges at the one-loop level is the quantum interference between both channels. Thus when the logarithmic diagrams are evaluated at zero external Peierls and Cooper variables, several diagrams cancel and only a $2k_{\rm F}$ electron-hole bubble remains for the renormalization of g_1 whereas g_2 is affected by a Cooper ladder graph. The remaining diagrams appear in Figure 2. After the outer shell integration, one obtains the one-loop scaling equations

$$\frac{\mathrm{d}\widetilde{g}_1}{\mathrm{d}l} = -\widetilde{g}_1^2$$

$$\frac{\mathrm{d}(2\widetilde{g}_2 - \widetilde{g}_1)}{\mathrm{d}l} = 0 \qquad (18)$$

where $\widetilde{g}_{1,2} \equiv g_{1,2}/\left(\pi v_{\rm F}\right)$. The combination of coupling constants $2\widetilde{g}_2 - \widetilde{g}_1$ is a renormalization group invariant which is related to the conservation of the particles on each branch for g_1 and g_2 scattering processes, when umklapp processes are neglected.

Another property of interest is that the decoupling of the above two scaling equations can be understood as a consequence of the separation between spin and charge long-wavelength degrees of freedom. This is clearly manifest when the Hamiltonian representation $H_I(l)$ of the effective interacting part of the action at step l is written in the Landau channel in a rotationaly invariant form

$$H_I[g_1(l),g_2(l)] = \sum_{p,q}(2g_2 - g_1)\rho_p(q)\rho_{-p}(-q) - g_1(l)$$

$$\times\sum_{p,q}\mathbf{S}_p(q)\cdot\mathbf{S}_{-p}(-q). \qquad (19)$$

Here the operators for the long-wavelength charge (ρ_p) and spin ($\mathbf{S}_p$) degrees degrees of freedom of branch p are respectively given, in operator form, by

$$\rho_{\pm p}(\pm q) = \frac{1}{2\sqrt{L}}\sum_{k,\sigma}^{*} c^{\dagger}_{\pm p,\sigma}(k)c_{\pm p,\sigma}(k\pm q)$$

$$\mathbf{S}_{\pm p}(\pm q) = \frac{1}{2\sqrt{L}}\sum_{k,\alpha\beta}^{*} c^{\dagger}_{\pm p,\alpha}(k)\boldsymbol{\sigma}_{\alpha,\beta}c_{\pm p,\beta}(k\pm q), \quad (20)$$

with the vector $\boldsymbol{\sigma}$ whose components are the usual Pauli matrices. Because of the integrated degrees of freedom, the summations on band wave vectors k are restricted to the interval $\mid \epsilon_p(k) \mid \leq E_0(l)/2$. This way of writing the effective Hamiltonian together with the scaling equations (4.1) emphasizes that interfering and logarithmically singular correlations of the Peierls and Cooper channels do influence uniform correlations of the Landau channel. This must be taken into account in the calculation of the uniform magnetic susceptibility as we show shortly.

Before concluding this subsection, we mention how g_4 appears in the partial trace operation equation (15). One can show that the coupling of g_1 and g_2 to g_4 at higher order also leads to logarithmic corrections to the vertex part which are equivalent to a renormalization of the Fermi velocity in the scaling equations (4.1). One then has $\tilde{g}_1 = g_1/(\pi v_\sigma)$ and $2\tilde{g}_2 - \tilde{g}_1 = (2g_2 - g_1)/(\pi v_\rho)$, where

$$v_{\rho,\sigma} = v_{\mathrm{F}}[1 \pm g_4(2\pi v_{\mathrm{F}})^{-1}]. \quad (21)$$

Here v_σ and v_ρ are respectively the velocity of spin and charge excitations. Thus for g_1 for example, one can write

$$g_1(l) = \frac{g_1}{1 + g_1(\pi v_\sigma)^{-1} l}, \quad (22)$$

while the charge coupling $2\tilde{g}_2 - \tilde{g}_1$ remains an invariant. As for the interaction term g_4 itself, it does not renormalize at this order [18].

4.2 Spin and charge susceptibilities from auxiliary fields

The renormalization described above is valid as long as the cut-off energy $E_0(l)/2$ is larger than the temperature. For smaller cut-off, the contributions from loop integrations are not logarithmic because of the Fermi occupation factors. While one could in principle modify the recursion relations to account for this and continue their integration [26], it is simpler to apply a sharp cut-off procedure. We simply use the effective action obtained for $l \approx \ln(E_{\mathrm{F}}/T)$ and apply perturbation theory to obtain the uniform susceptibility. We go through the exercise of formally generating the perturbative result through the auxiliary field (Hubbard-Stratonovich) method. This will allow us to exhibit the accuracy of standard perturbative techniques for a linearized spectrum in the Landau channel [6,11] and to find the infinite slope of the susceptibility in the zero temperature limit. But first, we must analyze the part of the Hamiltonian that we will take as the unperturbed one.

4.2.1 The g_4 theory

Rescaling wave vectors to recover the original units, all band momenta $|k|$ are now smaller than $\overline{k}_0 \approx T/v_{\mathrm{F}}$ and, correspondingly, transfer momenta $|q|$ have to be of the same order. Hence we are now working with a small cut-off theory involving only low-frequency, low-momentum interactions within a single branch. It will be useful then, later, to work in an interaction representation where in the zeroth-order Hamiltonian H_p^4 the two branches $\pm k_{\mathrm{F}}$ do not interact with each other.

$$\begin{aligned} H_p^4 = &\sum_{k,\sigma} \epsilon_p(k)\, c^{\dagger}_{p,\sigma}(k)\, c_{p,\sigma}(k) + \frac{g_4}{2L} \\ &\times \sum_{k,k'=-\overline{k}_0+pk_{\mathrm{F}}}^{\overline{k}_0+pk_{\mathrm{F}}} \sum_{q} \sum_{\sigma,\sigma'=\uparrow}^{\downarrow} c^{\dagger}_{p,\sigma}(k)\, c^{\dagger}_{p,\sigma'}(k') \\ &\times c_{p,\sigma'}(k'+q)\, c_{p,\sigma}(k-q)\,. \end{aligned} \quad (23)$$

We will need to know the value of averages such as $\left\langle S_{p\alpha}(\widetilde{q})\, S_{p'\alpha}(\widetilde{q}')\right\rangle_4$ computed with the above Hamiltonian. The label α refers to spatial direction, x, y, z, of the spin operator. Because the Hamiltonians H_p^4 are small cut-off Hamiltonians, the exact irreducible vertex in the particle-hole channel can be taken as g_4 without further Landau-theory-like renormalization from high-energy processes. A number of cancellations occur for this model [27], so that the final expression has an RPA like form,

$$\langle S_{p\alpha}(\widetilde{q})\, S_{p'\alpha}(\widetilde{q}')\rangle_4 \equiv \delta_{p,p'}\delta_{\widetilde{q},-\widetilde{q}'}\frac{1}{4}\frac{\chi_p^0(\widetilde{q})}{1 - \frac{1}{2}g_4\chi_p^0(\widetilde{q})}. \quad (24)$$

In this expression, the non-interacting susceptibility $\chi_p^0(\widetilde{q})$ on one branch branch $p = \pm$ is given by

$$\chi_p^0(\widetilde{q}) = -2\sum_k \frac{f[\epsilon_p(k)] - f[\epsilon_p(k+q)]}{\mathrm{i}q_n + \epsilon_p(k) - \epsilon_p(k+q)}, \quad (25)$$

where $f(\epsilon_p(k))$ is the Fermi function. At $\mathrm{i}q_n = 0$, this is one half of the total bare susceptibility since the sum over wave vectors is peaked near only one of the two Fermi points. At small wave vector and zero temperature,

$$\chi_p^0(q, \mathrm{i}q_n) = N(E_{\mathrm{F}})\frac{pv_{\mathrm{F}}q}{pv_{\mathrm{F}}q - \mathrm{i}q_n}, \quad (26)$$

with $N(E_{\mathrm{F}}) = (\pi v_{\mathrm{F}})^{-1}$ the bare density of states per branch (half of the total bare density of states). Similarly, the charge-charge correlation function is given by [27]

$$\langle \rho_p(\widetilde{q})\, \rho_{p'}(\widetilde{q}')\rangle_4 \equiv \delta_{p,p'}\delta_{\widetilde{q},-\widetilde{q}'}\frac{1}{4}\frac{\chi_p^0(\widetilde{q})}{1 + \frac{1}{2}g_4\chi_p^0(\widetilde{q})}. \quad (27)$$

Note that in the $\mathrm{i}q_n = 0$, $q \to 0$ limit we have at low temperature,

$$\begin{aligned} \lim_{q\to 0}\langle S_{p\alpha}(q,0)\, S_{p\alpha}(-q,0)\rangle_4 &= \frac{1}{4}\frac{(\pi v_{\mathrm{F}})^{-1}}{1 - g_4/(2\pi v_{\mathrm{F}})} \\ &\equiv \frac{1}{4}\frac{1}{\pi v_\sigma} \end{aligned} \quad (28)$$

$$\lim_{q\to 0}\langle\rho_p(q,0)\,\rho_p(-q,0)\rangle_4 = \frac{1}{4}\frac{(\pi v_{\rm F})^{-1}}{1+g_4/(2\pi v_{\rm F})} \equiv \frac{1}{4}\frac{1}{\pi v_\rho}, \tag{29}$$

where the spin and charge velocities are defined as above in equation (21).

4.2.2 Auxiliary-field representation

The magnetic susceptibility is obtained from a derivative with respect to an external magnetic field **h**. We choose units where the g factor times the Bohr magneton equals unity. In the presence of **h,** the partition function takes the form,

$$Z[\mathbf{h}] = {\rm Tr}\left\{ {\rm e}^{-\beta\left(H_+^4+H_-^4\right)}\, T_\tau\, \exp\left[-\int_0^\beta \left\{ H_I\left[g_1(l),g_2(l),\tau\right] - \Big(\sum_{p=\pm}\mathbf{S}_p(q,\tau)\Big)\cdot\mathbf{h}(-q,\tau)\right\}{\rm d}\tau\right]\right\}, \tag{30}$$

where we use the interaction representation in which the Hamiltonian H_p^4 studied in the previous section plays the role of the unperturbed Hamiltonian. Using Gaussian integration (Hubbard-Stratonovich decomposition), to decouple the interactions between branches, this may be rewritten as

$$\begin{aligned} Z = Z_4 \int\int \mathcal{D}\phi\mathcal{D}\mathbf{M} & \\ \times \exp\left(-\sum_q\sum_p \int_0^\beta {\rm d}\tau\, \left[\phi_p(q,\tau)\phi_{-p}(-q,\tau)\right.\right. & \\ \left.\left. + \mathbf{M}_p(q,\tau)\cdot\mathbf{M}_{-p}(-q,\tau)\right]\right) & \\ \times \left\langle T_\tau \exp\left(-\int_0^\beta {\rm d}\tau \mathcal{H}\left[\phi,\mathbf{M},\mathbf{h},\tau\right]\right)\right\rangle_4, & \end{aligned} \tag{31}$$

where ϕ and $\mathbf{M}$ are real auxiliary fields for charge and spin degrees of freedom respectively and

$$\mathcal{H}[\phi,\mathbf{M},\mathbf{h},\tau] = \sum_{p,q}\Big[2{\rm i}\sqrt{2g_2-g_1}\;\rho_p(q,\tau)\phi_p(-q,\tau) + 2\sqrt{g_1(l)}\,\mathbf{S}_p(q,\tau)\cdot\mathbf{M}_p(-q,\tau) - \mathbf{S}_p(q,\tau)\cdot\mathbf{h}(-q,\tau)\Big] \tag{32}$$

while $Z_4 \equiv {\rm Tr}\left[{\rm e}^{-\beta\left(H_+^4+H_-^4\right)}\right]$ and $\langle ...\rangle_4$ are respectively the partition function and corresponding averages calculated in the presence of the g_4 interaction only. As in previous sections, we use the following definition for quantities in Matsubara frequencies $\omega_m = 2\pi mT$, $m = 0, \pm1, \pm2, ...$

$$\mathbf{h}(\tau) = \sqrt{T}\sum_{\omega_m} {\rm e}^{-{\rm i}\omega_m\tau}\mathbf{h}(\omega_m) \tag{33}$$

$$\mathbf{h}(\omega_m) = \sqrt{T}\int_0^\beta {\rm d}\tau {\rm e}^{{\rm i}\omega_m\tau}\mathbf{h}(\tau). \tag{34}$$

With these definitions, and the change of variable $\mathbf{M}_p(\widetilde{q}) \to \mathbf{M}_p(\widetilde{q}) + \mathbf{h}(\widetilde{q})/\left(2\sqrt{g_1}\right)$, $\widetilde{q} = (q, \omega_m = 2\pi mT)$ the zero-field dynamic magnetic susceptibility per unit length can be formally expressed in terms of an average over the magnetic auxiliary field **M**, that is

$$\chi_\alpha(\widetilde{q}) = \left\langle \sum_{p,p'} S_{p\alpha}(\widetilde{q})\, S_{p'\alpha}(-\widetilde{q})\right\rangle = \left.\frac{\delta^2 \ln Z[\mathbf{h}]}{\delta h_\alpha(-\widetilde{q})\delta h_\alpha(\widetilde{q})}\right|_{\mathbf{h}=0} = \frac{1}{g_1(l)}[\langle\sum_p M_{p,\alpha}(\widetilde{q})\sum_{p'} M_{p',\alpha}(-\widetilde{q})\rangle - 1] \tag{35}$$

where the subscript α stands for the orientation of the magnetic field.

Applying the linked-cluster theorem in equation (31) and evaluating the averages $\langle\ldots\rangle_4$ using equations (28, 29) of the previous subsection allows one to write, in the rotationally invariant case,

$$Z = Z_4 \int\int \mathcal{D}\phi\mathcal{D}\mathbf{M}\exp\left\{ -\sum_{\widetilde{q},p,p\prime}\left[\phi_p(\widetilde{q})A_{p,p\prime}(\widetilde{q})\phi_{p\prime}(-\widetilde{q}) + \mathbf{M}_p(\widetilde{q})B_{p,p\prime}(\widetilde{q})\mathbf{M}_{p\prime}(-\widetilde{q})\right] + \mathcal{O}\left(\mathbf{M}^4,\phi^4,\mathbf{M}^2\phi^2\right)\right\} \tag{36}$$

with the matrix elements

$$A_{p,p}(\widetilde{q}) = \frac{1}{2}(2g_2-g_1)\frac{\chi_p^0(\widetilde{q})}{1+\frac{1}{2}g_4\chi_p^0(\widetilde{q})} \equiv \frac{1}{2}(2g_2-g_1)\chi_{c,p}^0(\widetilde{q}) \tag{37}$$

$$A_{+,-} = A_{-,+} = 1 \tag{38}$$

and

$$B_{p,p}(\widetilde{q}) = -\frac{1}{2}g_1(l)\frac{\chi_p^0(\widetilde{q})}{1-\frac{1}{2}g_4\chi_p^0(\widetilde{q})} \equiv -\frac{1}{2}g_1(l)\,\chi_{\sigma,p}^0(\widetilde{q}) \tag{39}$$

$$B_{+,-} = B_{-,+} = 1 \tag{40}$$

respectively for the charge and spin degrees of freedom of the Landau channel.

In these expressions, $g_1(l)$ is given by equation (22) with $l \approx \ln(\Lambda/T)$ where Λ is a cut-off of the order of the Fermi energy. Hence,

$$g_1(T) = \frac{g_1}{1+\frac{g_1}{\pi v_\sigma}\ln\frac{\Lambda}{T}}. \tag{41}$$

The neglect of mode-mode coupling or anharmonic terms in equation (36) is quite justified in one-dimension. Indeed we are in a low cut-off theory so that only the $\widetilde{q}=0$ components of the Hubbard-Stratonovich fields are important. When the unperturbed Hamiltonian is quadratic in fermion fields, the coefficients of the $\widetilde{q}=0$ mode-mode coupling terms vanish because they are derivatives of the density of states [28], a quantity that is a constant for a linear dispersion relation. For the same reason, the spatial rigidity of correlations of the auxiliary fields ϕ and **M** vanishes. Here the unperturbed part of the Hamiltonian is the interacting g_4 theory. It is known that in the theory with a linearized dispersion relation, the density fluctuations are

Gaussian, hence there is no mode-coupling term [27]. Furthermore, there is no singularity in this theory [29]. Here we will take into account the fact that the dispersion relation is not linear. This could make mode-mode coupling terms become different from zero at high temperature, far from the Luttinger liquid fixed point [13].

4.2.3 Susceptibilities

The Gaussian fluctuations of **M** evaluated with the functional equation (36) give us the magnetic susceptibility through equation (35). We find in the rotationaly invariant case

$$\chi(l) = \frac{1}{g_1(l)} \left(\frac{1}{2} \sum_{p,p'} \left(B^{-1} \right)_{p,p'} - 1 \right). \tag{42}$$

Using the expression equation (39) for $B_{p,p}$, one obtains,

$$\chi\left(\widetilde{q}\right) = -\frac{1}{4} \left[\frac{g_1\left(l\right) \chi^0_{\sigma,+}\left(\widetilde{q}\right) \chi^0_{\sigma,-}\left(\widetilde{q}\right) + \left(\chi^0_{\sigma,+}\left(\widetilde{q}\right) + \chi^0_{\sigma,-}\left(\widetilde{q}\right) \right)}{\frac{1}{4} g_1^2\left(l\right) \chi^0_{\sigma,+}\left(\widetilde{q}\right) \chi^0_{\sigma,-}\left(\widetilde{q}\right) - 1} \right]. \tag{43}$$

In the Luttinger-liquid limit, (linear dispersion relation) one finds for the retarded spin susceptibility,

$$\chi^R = -\frac{1}{4} \frac{2}{\pi v^s} \frac{\left(v^s q\right)^2}{\left(\omega + \mathrm{i}\eta\right)^2 - \left(v^s \widetilde{v}^s\right) q^2} \tag{44}$$

$$v^s = v_\sigma + \frac{g_1(l)}{2\pi} = v_{\mathrm{F}} - \frac{g_4}{2\pi} + \frac{g_1(l)}{2\pi} \tag{45}$$

$$\widetilde{v}^s = v_\sigma - \frac{g_1(l)}{2\pi} = v_{\mathrm{F}} - \frac{g_4}{2\pi} - \frac{g_1(l)}{2\pi} \tag{46}$$

which reduces to the known result [18,27] in the limit $g_1 = 0$.

For the static susceptibility of interest to us, the result is simpler. In that case, we take $\omega \to 0$ first and notice that

$$\chi^0_{\sigma,+}\left(q=0,\omega=0\right) = \chi^0_{\sigma,-}\left(q=0,\omega=0\right) \equiv \chi^0_p\left(T\right), \tag{47}$$

where $g_1\left(l\right)$ is evaluated at $l_T = \ln(E_{\mathrm{F}}/T)$. This leads to

$$\chi(T) = \frac{\frac{1}{2}\left(\frac{\chi^0_p(T)}{1 - \frac{1}{2} g_4 \chi^0_p(T)} \right)}{1 - \frac{1}{2} g_1(T) \left(\frac{\chi^0_p(T)}{1 - \frac{1}{2} g_4 \chi^0_p(T)} \right)}. \tag{48}$$

To leading order in $g_1(T)$, one finds

$$\chi(T) \approx \frac{1}{2} \chi^0_\sigma(T) [1 + \frac{1}{2} g_1(T) \chi^0_\sigma(T) + ...]$$

with

$$\chi^0_\sigma(T) \equiv \frac{\chi^0_p\left(T\right)}{1 - \left(2\pi v_{\mathrm{F}}\right)^{-1} g_4}. \tag{49}$$

In the absence of g_4, this expression, coincides with the result obtained previously by Dzyaloshinskii and Larkin [4] and by Lee *et al.* [5]. Our more general expression for the susceptibility equation (48) may be rewritten as

$$\chi(T) = \frac{\frac{1}{2} \chi^0_p(T)}{1 - \frac{1}{2}(g_4 + g_1(T)) \chi^0_p(T)}. \tag{50}$$

For the repulsive sector $g_1 > 0$, $g_1(T \to 0) \to 0$ is irrelevant in the zero temperature limit and there one recovers the Luttinger-liquid result [30],

$$\chi\left(T=0\right) = \left\langle \sum_{p,p'} S_{p\alpha}\left(0,0\right) S_{p'\alpha}\left(0,0\right) \right\rangle = \frac{1}{2\pi v_{\mathrm{F}} [1 - (2\pi v_{\mathrm{F}})^{-1} g_4]} = \frac{1}{2\pi v_\sigma}. \tag{51}$$

The analogous calculations for the charge fluctuations also lead to similar results. It suffices to do the following substitutions in any of the above spin susceptibility results:

$$g_4 \to -g_4 \tag{52}$$

$$g_1 \to g_1 - 2g_2. \tag{53}$$

In particular, in the static limit, the charge susceptibility $\chi_c\left(T\right)$ (or equivalently the isothermal compressibility $\kappa_T\left(T\right) = \chi_c\left(T\right)/n^2$) is given by

$$\chi_c\left(T\right) = \left\langle \sum_{p,p'} \rho_p\left(0,0\right) \rho_p\left(0,0\right) \right\rangle = \frac{\frac{1}{2}\chi^0_p}{1 + \frac{1}{2}(g_4 + 2g_2 - g_1)\chi^0_p(T)}. \tag{54}$$

Again in the repulsive sector $g_1 > 0$, $2g_2 - g_1$ is a renormalization group invariant when umklapp scattering can be neglected (*cf.* Eq. (18)) and one recovers the Luttinger-liquid result in the zero-temperature limit [30],

$$\chi_c\left(T=0\right) = \frac{1}{2\pi v_{\mathrm{F}} [1 + (2\pi v_{\mathrm{F}})^{-1} \left(g_4 + 2g_2 - g_1\right)]}. \tag{55}$$

4.2.4 Infinite slope in the zero temperature limit and third law of thermodynamics

While in the absence of umklapp scattering the charge susceptibility comes in the zero-temperature limit with zero slope, as in a Fermi liquid, the dependence of the magnetic susceptibility equation (50) on the marginally irrelevant variable $g_1\left(T\right)$ implies an infinite slope in the zero temperature limit. This can be seen as follows. Since $\partial\chi^0_p/\partial T$ has a finite limit as $T \to 0$, the singular contributions comes from

$$\frac{\partial \chi(T)}{\partial T} \to \chi^2(T) \frac{\partial g_1(T)}{\partial T}.$$

The temperature derivative of the marginally irrelevant variable equals infinity at $T = 0$ as can easily be obtained from the temperature derivative of equation (41)

$$\frac{\partial g_1(T)}{\partial T} = \frac{g_1}{\left(1 + \frac{g_1}{\pi v_\sigma} \ln \frac{A}{T}\right)^2} \frac{g_1}{\pi v_\sigma} \frac{1}{T}. \tag{56}$$

Hence,

$$\lim_{T\to o}\frac{\partial\chi(T)}{\partial T}=\infty. \tag{57}$$

A superficial look at the zero temperature infinite slope equation (57) suggests a violation of the third law of thermodynamics. Indeed, consider the grand potential $\Omega = E - TS - \mu N$, whose differential change is given by $\mathrm{d}\Omega = -S\mathrm{d}T - N\mathrm{d}\mu - \mathbf{M}\cdot\mathrm{d}\mathbf{B}$. Normalizing to unit volume on finds,

$$\frac{\partial}{\partial T}\chi\Big|_{T=0} = \frac{\partial}{\partial T}\frac{\partial M}{\partial B}\Big|_{T=0} = -\frac{\partial}{\partial T}\frac{\partial^2\Omega}{\partial B^2}\Big|_{T=0} \tag{58}$$

$$= -\frac{\partial^2}{\partial B^2}\frac{\partial}{\partial T}\Omega\Big|_{T=0} = \frac{\partial^2 S}{\partial B^2}\Big|_{T=0} = \infty. \tag{59}$$

The infinite second derivatives of the entropy seem to contradict the third law of thermodynamics that says that the entropy at zero temperature is independent of external parameters. However, because the point $T = 0$, $B = 0$ is a critical point (infinite correlation length), the free energy at this point is not analytic and we are not allowed to invert the order of differentiation as we did on the second line. Hence, one cannot conclude that $\frac{\partial}{\partial T}\chi\big|_{T=0} = \infty$ violates the third law [31]. The entropy of the Luttinger liquid does vanish at zero temperature, independently of B and μ [30].

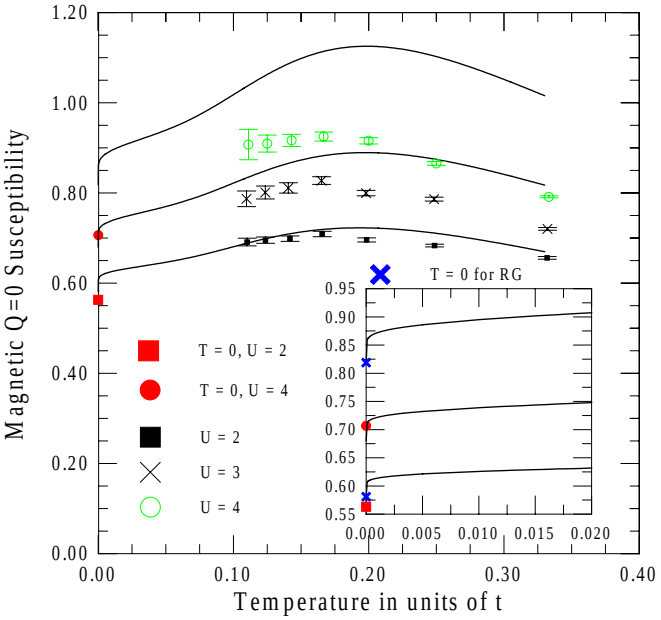

Fig. 3. Magnetic susceptibility χ evaluated from equations (48) or equivalently (50) with the naive replacements $g_4 = g_1 = U$ and, using equation (41), $g_1(T) = g_1/\left(1 + \frac{g_1}{\pi v_\sigma}\ln\frac{\Lambda}{T}\right)$ with $\Lambda = 2$. The spin velocity is obtained from equation (21), $v_{\rho,\sigma} = v_F[1 \pm g_4(2\pi v_F)^{-1}]$. The inset shows the low temperature region. In the inset, the X symbols show the low-temperature limit predicted by the RG.

5 Comparisons with Monte Carlo simulations

In this section, we shall compare the RG results first with the zero-temperature exact results and then with all the finite-temperature results exhibited in Figure 1. It is not yet possible to do simulations at low enough temperature to confirm or not the existence of the infinite slope seen in the RG approach in the $T \to 0$ limit since this also requires huge system sizes. It should however be possible to verify that regular extrapolation of finite T results to the $T = 0$ limit is not possible. At higher temperature and larger interaction strengths, non-logarithmic terms become important. We will show that it is possible to estimate these. In two dimensions, it has been possible to explain the complete temperature-dependent magnetic properties of the Hubbard model by using diagrammatic approaches [16,33] far from half-filling or the Two-Particle Self-Consistent approach [34,35] at arbitrary fillings. We briefly explore the predictions of these approaches in one-dimension. The reason for their failure in one dimension will help understand the correct way to proceed.

5.1 Comparisons with the renormalization group approach

To compare numerical Monte Carlo results with our RG results for the susceptibility equation (48) or equivalently equation (50), (remember the trivial factor of four to compare with simulations) one needs to know the initial values of g_1 and g_4 entering the scaling equations. As argued above, it is not strictly correct for the Hubbard model to assume that these constants can be taken as $g_1 = g_4 = U$ because the dispersion relation is not linear, and the cut-off in the initial model is not as in the g-ology model. Let us start by a comparison with the zero temperature exact results of Shiba. We find that our result equation (51) differs from that of Shiba by at most 15% up to $U = 4$ if we choose $g_4 = U$. At $U = 2$, the RG result is accurate to about 1%. The same conclusions were reached a long time ago in reference [32]. Hence, we conclude that at small coupling the estimate $g_1 = g_4 = U$ should be accurate.

To do a more general comparison at finite temperature, our results equations (41, 50) require in addition a value for the cut-off Λ. Taking $\Lambda = 2$, which corresponds roughly to half the bandwidth, of the order of the Fermi energy, produces the results in Figure 3. At low temperature, the results are not too sensitive to the value of Λ which enters only logarithmically. The comparison in Figure 3 shows that the disagreement with Monte Carlo results does become larger as U increases. Higher order logarithmic terms will not change the picture since they are smaller. As shown in the following subsections, the main source of discrepancy resides in non-logarithmic contributions that are actually not negligible at high temperature where the non-divergent (non-logarithmic) contributions dominate the magnetic susceptibility.

Let us discuss in turn the various features appearing in Figure 3. The Monte Carlo data shows that the temperature at which the maximum susceptibility occurs

is essentially independent of the interactions. The interactions determine only the overall enhancement and sharpness of the maximum but not the position. The position of the maximum $T_{\max}$ within RG also does not depend strongly on interactions but there can be a 10% shift in $T_{\max}$ when one changes the cut-off from $\Lambda = 1$ to $\Lambda = 2$. However, since the RG results do not seem very reliable near the maximum, we postpone this discussion to Section 5.5.

Decreasing the temperature from the position of the maximum, the RG predicts a first inflection point located at $T_i = 0.099 \pm 0.002$. This temperature is just at the limit of our Monte Carlo data. The inflection point can also not be seen in the more recent data of reference [8] since only the points $T = 0.1$ and $T = 0.05$ are available in the low-temperature region (see Fig. 1). This inflection point is again an effect that is caused by the band structure and within the above accuracy the position is independent of interactions. Indeed, while the curvature of the non-interacting susceptibility $\partial^2\chi_0/\partial T^2$ is negative at the maximum, it must be positive at low temperature because of the characteristics of the one-dimensional band with a parabolic bottom. The position of this inflection point is the same, within the quoted accuracy, whether one uses $\Lambda = 1$ or $\Lambda = 2$ or a temperature independent interaction as in Section 5.5. With a parabolic band instead of a cosine band, one finds an inflection point at $T_i = 0.101 \pm 0.002$, again essentially independent of cut-off or interactions.

Since the zero temperature value of the susceptibility is reached from finite temperature with an infinite slope, as discussed in the previous section, there is a second low-temperature inflection point. For $\Lambda = 2$, it appears at $T_L = 0.0329$, 0.0328, 0.0312 for, respectively, $U = 2, 3, 4$. This temperature is roughly three times lower than our lowest temperature in the Monte Carlo simulations and also lower than the other lowest available numerical results exhibited in Figure 1. The infinite slope in the susceptibility predicted by the RG appears confined to a small temperature range even when seen on a magnified scale, as one can check in the inset of Figure 3.

Contrary to the previous $T_{\max}$ and T_i, identified above, the location of the low-temperature inflection point T_L is not purely a band structure effect. It is clearly absent from $\chi_0(T)$. The low-temperature inflection point appears in the RG calculation because of the competition between the band-structure effects that lead to $\partial^2\chi_0/\partial T^2 > 0$ and the logarithmic singularity in $g_1(T)$ that leads to negative curvature in the full susceptibility at low temperature. As long as the interaction is sufficiently strong, this low-temperature inflection point occurs at a temperature that is remarkably independent of interactions. For lower values of the interaction, $U = 0.5$ and $U = 1$, one finds that the inflection point is at $T_L = 0.0208$ and $T_L = 0.0288$. Comparing with the above results, one sees that for $1 < U < 4$, the low-temperature inflection point is independent of interaction within about 10% ($T_L = 0.031 \pm 0.002$) while for $0.5 < U < 4$ the position varies from 0.02 to 0.03. The weak dependence on interaction comes from several factors: a) The interactions influence the susceptibility weakly, mainly to first order in the expansion of the RPA-like denominators. b) The inflection point occurs in a regime where $g_1(T)$ takes its asymptotic form, $\pi v_\sigma / \ln(\Lambda/T)$ which depends on the interactions only weakly through v_σ. c) Only the order T^2 of the Sommerfeld expansion of χ_0 suffices to obtain an accurate result. These three simplifications allow one to obtain an accurate analytical expression for the location of the inflection point. However, since terms up to order $T^2 \ln^3(\Lambda/T)$ must be kept, the resulting equation is transcendental and must be solved numerically.

The location of the low-temperature inflection point T_L clearly depends on the value of the cut-off Λ. However, since the dependence is logarithmic, the above results are not so sensitive to the precise value of the cut-off. For example, for $\Lambda = 1$ one finds $T_L = 0.0219$, 0.0304, 0.0349, 0.0345, 0.0324 for, respectively, $U = 0.5, 1, 2, 3, 4$. These values of T_L are larger than the corresponding values for $\Lambda = 2$ by at most 6%. For a parabolic band and $\Lambda = 2$, one finds $T_L = 0.035$, 0.035, 0.034 for $U = 2, 3, 4$ values that are at most 8% larger than the corresponding results for the cosine band with the same $\Lambda = 2$.

5.2 Diagrammatic Kanamori approach

From now on, we concentrate on the susceptibility at temperatures above the low-temperature inflection point, where the RG singularities do not contribute appreciably to the susceptibility. It was suggested long ago by Kanamori that the interaction appearing in RPA expressions should be renormalized. Following this idea, it was shown [16] that in two dimensions the renormalized $U_{\rm rn}$ can be accurately computed as follows:

$$U_{\rm rn} = \left\langle \frac{U}{1 + U\chi_{pp}(\mathbf{Q}, \mathrm{i}q_n = 0)} \right\rangle . \tag{60}$$

In this expression, the quantity $\chi_{pp}(\mathbf{Q}, \mathrm{i}q_n = 0)$ is the Cooper bubble for a total incident momentum $\mathbf{Q}$. The average is over the values of $\mathbf{Q}$. Several different types of averages can be done, namely over the whole Brillouin zone [16], or over wave vectors corresponding to values of $\mathbf{Q} = \mathbf{k} + \mathbf{k}'$ such that both $\mathbf{k}$ and $\mathbf{k}'$ are within an energy equal to the temperature T of the Fermi surface [36]. The latter type of approximation is closer in spirit to Fermi-liquid theory [37] and gives overall better results.

When the one-dimensional version of the procedure of reference [16] is applied to the present one-dimensional case, the agreement with the Monte Carlo results is apparently much better at high temperature than with the scaling approach. The temperature dependence is essentially correct and there is simply an underestimation of the overall magnitude of the susceptibility by 3%, 4%, and 9% for, respectively, $U = 2$, 3, and 4. The value of $U_{\rm rn}$ that we find may be approximated by

$$U_{\rm rn} \approx \frac{U}{1 + U\lambda} \tag{61}$$

with $\lambda \approx \langle \chi_{pp}(\mathbf{Q}, \mathrm{i}q_n = 0) \rangle \approx 0.29$.

In two dimensions, the agreement with Monte Carlo simulations is much better than found here and it is valid for all wave vectors, as long as the filling is such that there is no zero-temperature phase transition. In one dimension, the bare susceptibility at $q = 2k_{\rm F}$ diverges logarithmically with temperature at any filling because of nesting. This means that at sufficiently low temperature, RPA with a temperature and wave vector independent $U_{\rm rn}$ predicts a finite temperature phase transition at any filling. This is prohibited by the Mermin-Wagner theorem. Sure enough, for the values of U studied here, this transition occurs at a temperature much lower than those investigated above with Monte Carlo, but nevertheless, this is a question of principle that cannot be overlooked.

5.3 Two-particle self-consistent approach (TPSC)

The TPSC approach [34,35] avoids any finite-temperature phase transition in both one and two-dimensions. Hence, we may check wether this gives a better agreement with Monte Carlo simulations than the previous approach. The one-dimensional version of the theory can be summarized as follows. One approximates spin and charge susceptibilities $\chi_{\rm sp}$, $\chi_{\rm ch}$ by RPA-like forms but with two different effective interactions $U_{\rm sp}$ and $U_{\rm ch}$ which are then determined self-consistently using sum rules. Although the susceptibilities have an RPA functional form, the physical properties of the theory are very different from RPA because of the self-consistency conditions on $U_{\rm sp}$ and $U_{\rm ch}$. The necessity to have two different effective interactions for spin and for charge is dictated by the Pauli exclusion principle $\langle n_\sigma^2\rangle = \langle n_\sigma\rangle$ which implies that both $\chi_{\rm sp}$ and $\chi_{\rm ch}$ are related to only one local pair correlation function $\langle n_\uparrow n_\downarrow\rangle$. Indeed, using the fluctuation-dissipation theorem in Matsubara formalism and the Pauli principle one can write:

$$\frac{1}{\beta N}\sum_{\widetilde{q}}\chi_{\rm ch}(\widetilde{q}) = n + 2\langle n_\uparrow n_\downarrow\rangle - n^2 = \frac{1}{\beta N}\sum_{\widetilde{q}}\frac{\chi_0(\widetilde{q})}{1+\frac{1}{2}U_{\rm ch}\chi_0(\widetilde{q})}, \qquad (62)$$

$$\frac{1}{\beta N}\sum_{\widetilde{q}}\chi_{\rm sp}(\widetilde{q}) = n - 2\langle n_\uparrow n_\downarrow\rangle = \frac{1}{\beta N}\sum_{\widetilde{q}}\frac{\chi_0(\widetilde{q})}{1-\frac{1}{2}U_{\rm sp}\chi_0(\widetilde{q})}, \qquad (63)$$

where $\beta \equiv 1/T$, $n = \langle n_\uparrow\rangle + \langle n_\downarrow\rangle$, $\widetilde{q} = (q, {\rm i}q_n)$ with q the wave vectors of an N site lattice, ${\rm i}q_n$ Matsubara frequencies and $\chi_0(\widetilde{q})$ the susceptibility for non-interacting electrons. The first equalities in each of the above equations is an exact sum-rule, while the last equalities define the TPSC approximation for $\chi_{\rm ch}(\widetilde{q})$ and for $\chi_{\rm sp}(\widetilde{q})$. In this approach, the value of $\langle n_\uparrow n_\downarrow\rangle$ may be obtained self-consistently [34] by adding to the above set of equations the relation $U_{\rm sp} = g_{\uparrow\downarrow}(0)\,U$ with $g_{\uparrow\downarrow}(0) \equiv \langle n_\uparrow n_\downarrow\rangle/\langle n_\downarrow\rangle\langle n_\uparrow\rangle$. As shown in reference [34], the above procedure reproduces both the Kanamori-Brueckner screening described in the previous section as well as the effect of Mermin-Wagner thermal fluctuations, giving a phase transition only at zero-temperature in two dimensions. In two dimensions, there is however a crossover temperature T_X below which the magnetic correlation length ξ can grow exponentially. Quantitative agreement with Monte Carlo simulations is obtained [34] for all fillings and temperatures in the weak to intermediate coupling regime $U < 8t$. The equation (62) for charge is not necessary to obtain the spin structure factor.

In one dimension, the absence of phase transition in this theory at finite temperature can be proven as follows. Near the temperature at which the phase transition would occur in RPA, $\delta U \equiv U_{\rm mf,c} - U_{\rm sp} \approx 0$, ($U_{\rm mf,c} \equiv 2/\chi_0\,(2k_{\rm F},0)$) the $q = 2k_{\rm F}$ susceptibility at zero Matsubara frequency is becoming very large so that the self-consistency relation equation (63) can be approximated by

$$2T\int\frac{{\rm d}q}{2\pi}\frac{2}{U_{\rm sp}\xi_0^2(\xi^{-2}+q^2)} = n - 2\langle n_\uparrow n_\downarrow\rangle - C, \qquad (64)$$

where

$$\xi_0^2 \equiv \frac{-1}{2\chi_0\,(q)}\left.\frac{\partial^2\chi_0\,(q,0)}{\partial^2 q}\right|_{q=2k_{\rm F}} \qquad (65)$$

$$\xi \equiv \xi_0(U_{\rm sp}/\delta U)^{1/2}, \qquad (66)$$

and where the integral is for q around $2k_{\rm F}$ or $-2k_{\rm F}$ and C contains contributions from non-zero Matsubara frequencies and from corrections to the Lorentzian approximation used for the ${\rm i}q_n = 0$ contribution. Then,

$$\frac{4T}{U_{\rm sp}\xi_0^2}\int\frac{{\rm d}q}{2\pi}\frac{1}{\xi^{-2}+q^2} \approx \frac{4T}{U_{\rm sp}\xi_0^2}\xi = n - 2\langle n_\uparrow n_\downarrow\rangle + C. \qquad (67)$$

Since the right-hand side is a finite number, ξ behaves as $U_{\rm sp}\xi_0^2/\,(4T)$, becoming infinite at zero temperature only. There is however nothing to prevent a zero-temperature phase transition in the theory, so that it cannot describe accurately the one-dimensional systems at very low temperature.

Comparisons with the Monte Carlo simulations reveal discrepancies of order 25% for the case $U = 4$. This means that contrary to the two-dimensional case, this approach does not even reproduce well the Kanamori-Brueckner result described in the previous section. If we had taken $\langle n_\uparrow n_\downarrow\rangle$ from Monte Carlo data in the sum rule equation (63) instead of computing it self-consistently from the *ansatz* $U_{\rm sp} = U\langle n_\uparrow n_\downarrow\rangle/\langle n_\downarrow\rangle\langle n_\uparrow\rangle$ the results would have been much better. In other words, the calculation of $\langle n_\uparrow n_\downarrow\rangle$ self-consistently is an assumption that fails in one dimension even more drastically than the RPA functional form with an effective $U_{\rm sp}$. The whole approach fails completely at low temperature. Indeed $U_{\rm mf,c} \equiv 2/\chi_0\,(2k_{\rm F},0)$ vanishes as $T \to 0$ while $\delta U \equiv U_{\rm mf,c} - U_{\rm sp}$ has to remain positive according to the above arguments. This in turn implies that $U_{\rm sp}$ tends to zero at zero temperature which

means that the uniform magnetic susceptibility would not be enhanced at zero-temperature with this theory, contrary to both exact and renormalization group results. One could have hoped to use this approach to evaluate non-logarithmic contributions at high temperature and inject them in the RG expression, but in fact the logarithmic temperature dependence of the susceptibilities starts at rather high temperature.

5.4 General reason for the failure of higher-dimensional approaches

All of the above approaches fail for several reasons. They do not take into account the destructive interference between Cooper and Peierls channels and they try to describe the whole q dependence of the susceptibility with a single wave-vector-independent effective interaction $U_{\rm sp}$ or $U_{\rm rn}$. This is very different from the scaling theory which clearly shows that the effective interaction near $q = 0$ is different from that near $q = 2k_{\rm F}$.

The fact that the magnetic susceptibility in one-dimension cannot be described with a single wave vector independent effective interaction $U_{\rm sp}$ or $U_{\rm rn}$ is illustrated in Figure 4a. The simulations are taken from reference [32]. The solid lines are for an RPA-like form

$$\frac{\chi_0(q,0)}{1-\frac{1}{2}U\chi_0(q,0)} \tag{68}$$

and the data is normalized by $\chi_0(q,0)$ as in reference [32]. While the bare value for the simulation is $U = 2$, one needs a renormalized value $U = 1.3$ to fit the components near $q = 0$, while to fit near $q = 2k_{\rm F}$ one needs $U = 1.7$. Note also that the simulations are done for the canonical ensemble so that the $q = 0$ component is strictly zero and is not shown.

The magnetic structure factor contains not only the above susceptibility, but also all the non-zero Matsubara frequency components of the susceptibility. That is why it is less sensitive to the $\pm 2k_{\rm F}$ effects of one dimension. As illustrated in Figure 4b, the Monte Carlo data of reference [32] for $U = 2$ can this time be fitted, misleadingly, with a single renormalized $U = 1.5$.

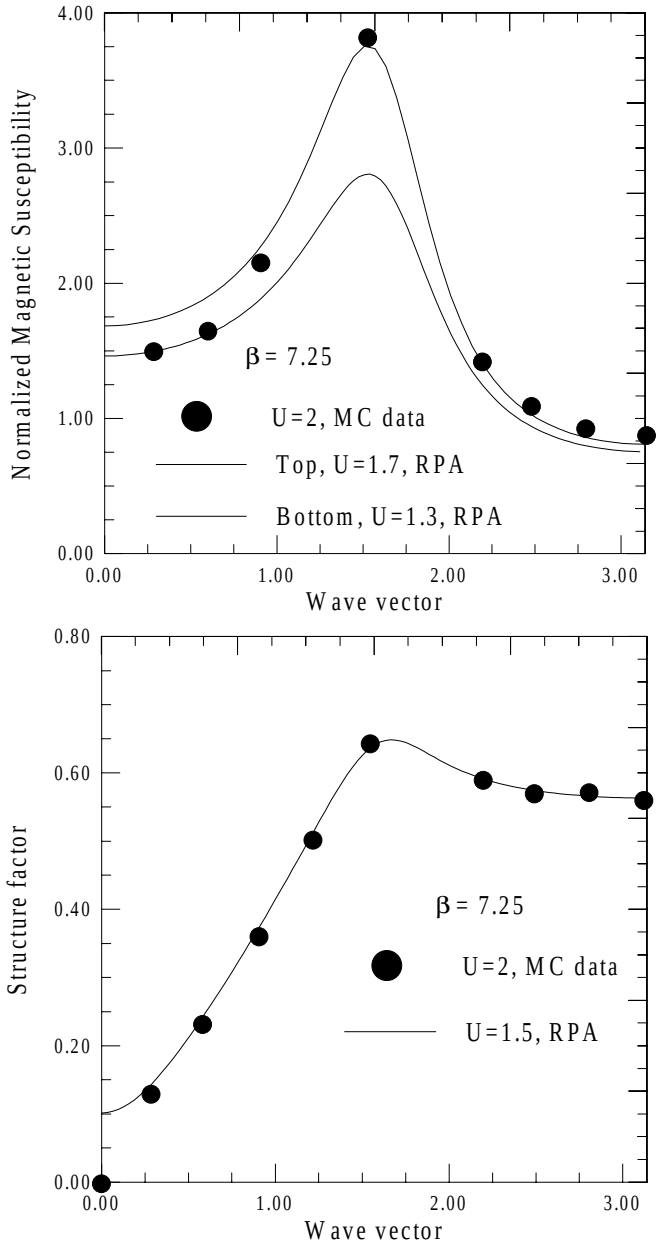

Fig. 4. a) Magnetic susceptibility $\chi(q)$ as a function of wave vector, normalized to its non-interacting $q = 0$ value. The Monte Carlo data is from reference [32]. The solid lines illustrate that when the whole q dependence is considered, RPA fits are inadequate, even with renormalized values of the interaction. b) Magnetic structure factor equation (8) as a function of wave vector, $S(q)$. The Monte Carlo data is from reference [32]. The solid line illustrates that this time, as opposed to part (a), a simple RPA fit with a renormalized value of U may work misleadingly well.

5.5 Modified-Kanamori approach in one dimension

In the renormalization group description of magnetic fluctuations, it is clear that the effective interactions near $q = 0$ and near $q = 2k_{\rm F}$ are different. No finite or zero-temperature phase transition occurs even though the uniform magnetic susceptibility is enhanced. However, this approach takes into account only logarithmic terms and applies only in the vicinity of either $q = 0$ or $q = 2k_{\rm F}$. It does not allow one to draw the full q-dependent susceptibility appearing in Figure 4 for example. Furthermore, we have seen that the renormalization group result for $q = 0$ becomes inaccurate compared with Monte Carlo simulations at high temperature. This can be understood as follows. In addition to the fact that we have employed an approximate sharp cut-off procedure, we do not know the exact value of g_4 and of g_1 entering the recursion relations. But more importantly, logarithmic terms are less singular at high temperature so that non-logarithmic terms also become important. To estimate non-logarithmic contributions, we proceed as follows.

In the same spirit as the Kanamori approach in higher dimensions, we want to find an effective interaction that contains the effect of other channels. This time however, the effective interaction should be valid only for $q \sim 0$. The RG result suggests that it is the contribution from the particle-hole channel that is important. Indeed, g_1 entering the expressions (48, 50) for the susceptibility contains the set of all diagrams generated by summing $2k_{\mathrm{F}}$ electron-hole bubbles [11]. This can be seen from Figure 2 and from the recursion relation equation (4.1). In Figure 2, all cross terms involving $g_1 g_2$ cancel each other in the cut-off theory so that only the g_1^2 contribution represented by the bubble is left. This shows that in the RG approach only $2k_{\mathrm{F}}$ electron-hole contributions are important. In the computation of the magnetic susceptibility however, one can observe that internal summations over all momentum transfers are present (including $q = 0$ where electron-hole bubbles are also the only type of diagrams that contribute in the calculation of χ for H_p^4 [18,27]). In order to include these non-logarithmic effects in the calculation of the susceptibility we average the resummed series of electron-hole bubbles over the entire Brillouin zone. More specifically, we take

$$U_m = \left\langle \frac{U}{1 + U\chi_{eh}\left(q, \mathrm{i}q_n = 0\right)} \right\rangle_q , \tag{69}$$

with

$$\chi_{\mathrm{eh}}\left(q, \mathrm{i}q_n = 0\right) = -N^{-1} \sum_k \frac{f\left[\epsilon\left(k-q\right)\right] - f\left[\epsilon\left(k\right)\right]}{\epsilon\left(k-q\right) - \epsilon\left(k\right)}.$$

Here the full effect of the lattice is restored by taking $\epsilon\left(k\right) = -2t\cos k$ with the summation over k that covers the entire Brillouin zone $[-\pi, \pi]$. It is clear from this procedure that for $|q| \approx 0$, the average will contribute to a g_4 type of process while for $\mid q \mid \approx 2k_{\mathrm{F}}$ the contribution will be to a g_1 type of process, as suggested by equation (50). One can also check that the Cooper and Peierls-type of bubble diagram, such as those appearing in $g_1 g_2$ processes in Figure 2, do cancel at half-filling when averaged over the Brillouin zone. At this filling, there is perfect particle-hole symmetry, even with a $2t\cos k$ dispersion relation. Even if this cancellation is no longer strictly valid away from half-filling, we write

$$\chi(T) = \frac{\chi_0(q,0)}{1 - \frac{1}{2}U_m\chi_0(q,0)} \tag{70}$$

for the total susceptibility with U_m computed from equation (69).

The results for the susceptibility are compared with the Monte Carlo results in Figure 5. The agreement is within the statistical uncertainty except near $T = 0.33$. As in the Kanamori approach, for the range of temperatures illustrated in Figure 5 we can approximate U_m by a temperature-independent value given by

$$U_m = \frac{U}{1 + U\lambda_m} \tag{71}$$

with $\lambda_m = \left\langle \Lambda_m\left(q, \mathrm{i}q_n = 0\right)\right\rangle_q$. This last approximation gives, within about 2% in the worse case, the same value

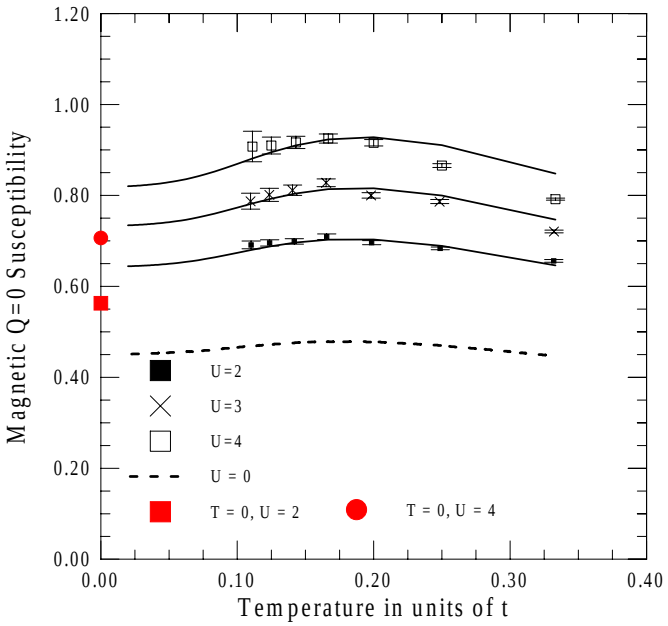

Fig. 5. Numerical results for the temperature dependent susceptibility, as already illustrated in Figure 1, compared with the Modified-Kanamori approach defined by an RPA from with a renormalized value of the interaction U_m given as a function of the bare value U by equations (69) or (71).

for the susceptibility as that obtained from equation (69). Using the low temperature value, $\lambda_m \simeq 0.25$, over the full temperature range improves the agreement near $T = 0.33$. At $T = 0$ the above modified-Kanamori approach overestimates the exact result by 13% at $U = 2$ and by as much as 17% for $U = 4$ showing clearly that a Fermi-liquid like extrapolation of the finite-temperature data does not yield the correct zero-temperature limit, as should be clear from Figure 5. Independently of the RG then, it seems certain that a change in curvature is needed to extrapolate to the correct zero-temperature limit. The RG result [32] with $g_4 = U$ on the other hand does have a change in curvature below $T = 0.1$ and extrapolates to the exact $T = 0$ result [22] to within 1% for $U = 2$ and makes physical sense even if 15% deviations occur in the extrapolation around $U = 4$.

Within the approach we just discussed, we can now come back to the question of the location of the maximum in the spin susceptibility. The Monte Carlo data suggests that the location of the maximum is essentially independent of interaction, a result that is an obvious consequence of the analytical form of the susceptibility that we used when U_{rn} has a temperature dependence that can be neglected. We find that $T_{\max} = 0.178$ is determined purely by the band structure and at quarter filling is even the same at the 1% level for a cosine or a parabolic band. Nevertheless, we do not have a simple analytical expression for the position of the maximum. Indeed, a Sommerfeld expansion of χ_0 up to order T^6 predicts that χ_0 always increases with temperature. It is the competition of this increase with the eventual Curie-Weiss decrease

of the susceptibility at high temperature that produces the maximum. The Curie-Weiss decrease is beyond the radius of convergence of the Sommerfeld expansion.

To extract the strength of interactions from a measurement of $\chi(T)$ one would need to know the bare value of $\chi_0(T)$. When $\chi_0(T)$ is unknown, one measure of the strength of interactions that suggests itself, given the position of the maximum $T_{\max}$ and of the high-temperature inflection point T_i is $R = (\chi(T_{\max}) - \chi(T_i))/\chi(T_{\max})$. In percentage, one finds, for $U = 2$ and $U = 4$, respectively, $R = 4.2\%$ and 5.2%. Unfortunately it turns out that this result is too sensitive to the band structure to really be useful in practice since for a parabolic band the above cosine band results are replaced by $R = 3.7\%$ and 4.5%.

6 Discussion and conclusion

We have shown in this paper that the temperature-dependent magnetic spin susceptibility of the Hubbard model at quarter-filling has the following general features in the weak to intermediate coupling regime ($0 < U < 4t$). As temperature is decreased, one encounters a maximum in the susceptibility at $T_{\max} \sim 0.18t$ that arises from the competition between the Curie-Weiss high-temperature decrease and the low temperature increase caused by the proximity to the characteristic van Hove singularity of one-dimensional systems with a parabolic band bottom. Decreasing the temperature, there is then an inflection point at $T_i \sim 0.1t$. The position of the maximum and of the inflection point are essentially independent of interaction strength, as confirmed by Monte Carlo simulations. Although a rough measure of the strength of the interactions may be obtained by comparing the relative size of the susceptibility at the maximum and at the inflection point this is not very reliable since one needs high accuracy as well as rather detailed information on the band structure: Indeed, a ratio $(\chi(T_{\max}) - \chi(T_i))/\chi(T_{\max})$ of order 4% may correspond to either $U \sim 4t$ or $U \sim 2t$ depending on whether the band structure is parabolic or cosinusoidal. As shown in Figure 5, the magnetic susceptibility curve obtained from Monte Carlo simulations between $T \sim 0.1t$ and $T \sim 0.33t$ may be reproduced very simply by an RPA-like form with an effective interaction U_m for the $q = 0$ component of the susceptibility. For the case considered here, one finds $U_m = U/(1 + U\lambda_m)$ with $\lambda_m \sim 0.25$. That effective interaction may be computed from the bare one using the subset of diagrams that naturally appears in the RG calculation. This effective interaction allows one to take into account non-logarithmic corrections that are beyond the RG approach. The effective interaction is valid only near $q = 0$. Approaches to the interacting problem that work in dimensions larger than $d = 1$ fail essentially because they keep an RPA form for all values of q, an approximation that is incorrect in one-dimension because of the destructive interference that occurs between $q = 2k_{\mathrm{F}}$ Peierls and $q = 0$ Cooper channels.

At $T = 0$, the logarithmic terms in the leading marginally irrelevant operator of the RG lead to an infinite slope $\partial\chi/\partial T$. This Luttinger-liquid result is strikingly different from the Fermi liquid prediction $\partial\chi/\partial T = 0$ at $T = 0$. Figure 5 clearly shows that a Fermi-liquid extrapolation of the finite-temperature data to the $T = 0$ exact result is inappropriate. The RG approach that we used also allows to show that in the presence of band structure effects (parabolic band bottom) the appearance of the Luttinger-liquid regime at low temperature is signaled by a low-temperature inflection point located at $T_L = (0.031 \pm .002)t$ for $t \leq U \leq 4t$ and $\Lambda = 2t$. Although the near independence of T_L on the precise value of the interactions for sufficiently large bare U does not have a simple origin, as discussed in Section 5.1, it comes in large part from the fact that in this case T_L occurs in a regime where the marginally irrelevant interaction takes its asymptotic form $\pi v_\sigma/\ln(\Lambda/T)$. This form depends on interactions only weakly through v_σ. The location of T_L is also not so sensitive to the (unkown) value of the cut-off since for $\Lambda = t$ one finds that T_L is larger than the corresponding values for $\Lambda = 2t$ by at most 6% over the whole range $0.5t \leq U \leq 4t$. For $\Lambda = 2t$, T_L can also be larger by at most 8% for a parabolic band compared with a cosine band. The above Luttinger-liquid regime $\left(\text{where } \partial^2\chi/\partial T^2 < 0\right)$ occurs at a temperature lower than what has been achieved by numerical calculations up to now. It is quite a challenge to verify them. It is also important to realize that even though the logarithmic Luttinger-liquid limit shows up in the spin susceptibility at quite low temperature, logarithmic contributions do appear at higher temperature in other quantities such as the longitudinal spin relaxation time T_1.

Although our results are for the quarter-filled model, it is clear that all the qualitative features should hold for fillings that are not too close to half-filling. A good quantitative estimate for the location of the characteristic features of the temperature-dependent spin susceptibility can easily be obtained for any other filling using the simple analytical expressions that we have found in Sections 4.2 and 5.5. Our analytical expressions may also be used to compute the charge susceptibility (compressibility), which as we saw has no singularity in the $T \to 0$ limit, as long as umklapp scattering can be neglected [38]. One could also use our approach to make quantitative predictions for more general models than the Hubbard model. Comparisons with experiment should help to establish appropriate bare microscopic parameters for the Hamiltonians of one-dimensional organic conductors.

We are grateful to S. Moukouri for useful discussions and to G. Jüttner for sending data. We acknowledge the support of the Natural Sciences and Engineering Research Council of Canada (NSERC), the Fonds pour la formation de chercheurs et l'aide à la recherche from the Government of Québec (FCAR), the Centre d'Applications du Calcul Parallèle de l'Université de Sherbrooke for the use of an IBM-SP2.

References

1. C. Bourbonnais in *Strongly-interacting Fermions and High-temperature Superconductivity,* edited by B. Douçot, J. Zinn-Justin (North Holland, Amsterdam, 1995), pp. 307-369.
2. P. Wzietek, F. Creuzet, C. Bourbonnais, D. Jérome, K. Bechgaard, P. Batail, J. Phys. I France **3**,171 (1993).
3. J. Voit, Rep. Prog. Phys. **58,** 977 (1995).
4. I.E. Dzyaloshinskii, A.I. Larkin, Sov. Phys. JETP **34**, 422 (1972).
5. P.A. Lee, T.M. Rice, R. Klemm, Phys. Rev. B **15**, 2984 (1977).
6. C. Bourbonnais, J. Phys. I France **3**, 143 (1993).
7. T. Usuki, N. Kawakami, A. Okiji, J. Phys. Soc. Jap. **59**, 1357 (1990); N. Kawakami, T. Usuki, A. Okiji, Phys. Lett. A **137**, 287 (1989).
8. G. Jüttner, A. Klümper, J. Suzuki, Nucl. Phys. B **522**, 471 (1998).
9. F. Mila, K. Penc, Phys. Rev B **51**, 1997 (1995).
10. S. Moukouri, L.G. Caron in *Density-Matrix Renormalization, a New Numerical Method in Physics*, edited by I. Peschel, X. Wang, M. Kaulke, K. Hallberg (Springer-Verlag, 1999).
11. H. Nélisse, MSc Thesis, Université de Sherbrooke, III-743, (1992).
12. S. Eggert, I. Affleck, M. Takahashi, Phys. Rev. Lett. **73**, 332 (1994).
13. B. Dumoulin, C. Bourbonnais, S. Ravy, J.P. Pouget, C. Coulon, Phys. Rev. Lett. **76**, 1360 (1996).
14. J. Kanamori, Prog. Theor. Phys. **30,** 275 (1963).
15. K.A. Brueckner, C.A. Levinson, Phys. Rev. **97**, 1344 (1955); K.A. Brueckner, J.L. Gammel, Phys. Rev. **109,** 1023, 1040 (1958).
16. Liang Chen, C. Bourbonnais, T. Li, A.-M.S. Tremblay, Phys. Rev. Lett. **66**, 369 (1991).
17. I.E. Dzyaloshinskii, A.I. Larkin, Sov. Phys. JETP **34**, 422 (1972); Y. Bychkov, L.P. Gor'kov, I.E. Dzyaloshinskii, Sov. Phys. JETP **23**, 489 (1966).
18. J. Solyom, Adv. Phys. **28**, 201 (1979).
19. V.J. Emery, in *Highly Conducting one-dimensional Solids*, edited by J.T. Devreese, R.P. Evrard, V.E. van Doren (Plenum, New York, 1979), p. 247.
20. Y.A. Firsov, V.N. Prigodin, Chr. Seidel, Phys. Rep. **126**, 245 (1985).
21. C. Bourbonnais, L.G. Caron, Int. J. Mod. Phys. B **5**, 1033 (1991); C. Bourbonnais, L.G. Caron, Europhys. Lett. **5,** 209 (1988); Physica B **143,** 451 (1986).
22. H. Shiba, Phys. Rev. B **6**, 930 (1972).
23. R. Blankenbecler, D.J. Scalapino, R.L. Sugar, Phys. Rev. D **24**, 2278 (1981); J.E. Hirsch, Phys. Rev. B **31**, 4403 (1985); S.R. White, D.J. Scalapino, R.L. Sugar, E.Y. Loh, J.E. Gubernatis, R.T. Scalettar, Phys. Rev. B **40**, 506 (1989); For a review, see E.Y. Loh, J.E. Gubernatis, in *Electron Phase Transitions*, edited by W. Hauke, Y.V. Kopaev (Elsevier, Amsterdam, 1992), pp. 177-235.
24. M. Suzuki, Phys. Lett. A **113**, 299 (1985); R.M. Fye, Phys. Rev. B **33**, 6271 (1986); R.M. Fye, R.T. Scalettar, Phys. Rev. B **36**, 3833 (1987).
25. K.B. Blagoev, K.S. Bedell, Phys. Rev. Lett. **79**, 1106 (1997).
26. G.Y. Chitov, D. Sénéchal, Phys. Rev. B. **52**, 13487 (1995).
27. W. Metzner, C. Di Castro, Phys. Rev. B **47**, 16107 (1993).
28. J.A. Hertz, Phys. Rev. B **14**, 1165 (1976).
29. The singularity of the uniform susceptibility at $g_4/(2\pi v_{\rm F}) = 1$ is beyond the weak coupling regime. Our approach is not valid in the strong-coupling regime.
30. H.J. Schulz, Phys. Rev. Lett. **64**, 2831 (1990); Int. J. Mod. Phys. B **5**, 57 (1991).
31. S. Eggert, oral communication.
32. J.E. Hirsch, D.J. Scalapino, Phys. Rev. B **27**, 7169 (1983).
33. N. Bulut, D.J. Scalapino, S.R. White, Phys. Rev. B **47**, 2742 (1993).
34. Y.M. Vilk, Liang Chen, A.-M.S. Tremblay, Phys. Rev. B **49**, 13 267 (1994).
35. Y.M. Vilk, A.-M.S. Tremblay, Europhys. Lett. **33**, 159 (1996); Y.M. Vilk, A.-M.S. Tremblay, J. Phys. I France, **7**, 1309 (1997).
36. D. Groleau, MSc thesis, Université de Sherbrooke, III-729 (1992).
37. See Appendix C of A.-M. Daré, L. Chen, A.-M.S. Tremblay, Phys. Rev. B **49**, 4106 (1994).
38. When the band-filling is commensurate, *e.g.* at quarter-filling, one expects logarithmic transients in the RG flow of the charge coupling $2g_2 - g_1$. These transients should also lead to an infinite slope at $T = 0$ as for the magnetic susceptibility. These transients get weaker in amplitude as the order of commensurability increases. See for example T. Giamarchi, Physica B **230-232**, 975 (1997).